Journal of Applied Fluid Mechanics, Vol. 11, No. 1, pp. 43-53, 2018.
Available online at www.jafmonline.net, ISSN 1735-3572, EISSN 1735-3645.
DOI: 10.29252/jafm.11.01.27715

Effects of Reinjection on Flow Field of Open Jet Automotive Wind Tunnel Test Section

Q. Li[1,2†], W. Dai[1,2], L. Zhong[1,2], Z. Yang[1,2], K. Du[1,2], Y. Xu[1,2] and M. M. Rashidi[3]

[1]*Shanghai Automotive Wind Tunnel Center, Tongji University, Shanghai, China*
[2]*Shanghai Key Lab of Vehicle Aerodynamics and Vehicle Thermal Management Systems，Shanghai, China*
[3]*Department of Civil Engineering, School of Engineering, University of Birmingham, Birmingham, UK*

†*Corresponding Author Email: qiliang.li@sawtc.com*

(Received February 23, 2017; accepted September 9, 2017)

ABSTRACT

The distributions of axial static pressure coefficient and flow fluctuation in the test section which affect aerodynamic measurement in an open jet wind tunnel is presented. In this paper, the flow characteristics of the open jet automotive wind tunnel with passive reinjection and active reinjection were simultaneously investigated by experimental and numerical approaches. The axial static pressure coefficient variations can be reduced by passive or active reinjection, and recycle flow returns to the test section from the loophole is the main reason. The more mass flow rate improves the effect. Meanwhile, it is found that the improvement of the axial static pressure coefficient by reinjection is always better in the condition of 0° collector angle. The turbulence intensity in the collector angle of 15° is lower than that of 0°, and the reinjection increases the turbulence intensity near the collector. The increase of the turbulence intensity by active reinjection in the collector angle of 0° is greater than the collector angle of 15° for the 3.28° diffusion angle. There are some peaks emerging at the frequencies of 40 Hz and 50 Hz, which indicates that the flow field fluctuations may have induced structural vibration. The peaks at several frequencies increase when the passive and active reinjection are conducted, and the increase of peak is correlate with the increase of the reinjection flow rate. Due to the reduction of average static pressure coefficient and increase of flow fluctuations, the application of passive and active reinjection should be considered at the same time.

Keywords*:* Open jet automotive wind tunnel; Axial static pressure coefficient; Turbulence intensity; Velocity and pressure fluctuations.

NOMENCLATURE

C_1	constant
$C_{1\varepsilon}$	constant
C_2	constant
$C_{3\varepsilon}$	constant
C_{pi}	local static pressure coefficient
G_k	the generation of turbulence kinetic energy due to the mean velocity gradients
G_b	the generation of turbulence kinetic energy due to buoyancy
k	turbulence kinetic energy
L	length of 1:15 scale vehicle
P_i	local static pressure
P_{ref}	reference static pressure
P_{0d}	dynamic pressure
PSD	power spectral density
S_k	user-defined source terms
t	time
u_j	j direction velocity, j = 0,1,2
x/L	dimensionless measurement point coordinate
Y_M	the contribution of the fluctuating dilatation in compressible turbulence to the overall dissipation rate
$y+$	dimensionless wall distance
σ_ε	the turbulent Prandtl numbers for ε
ρ	density
ν	kinematic viscosity
μ	dynamic viscosity
μ_t	dynamic viscosity of turbulence
σ_k	the turbulent Prandtl numbers for k
ε	dissipation rate

1. INTRODUCTION

Automotive wind tunnel is an important test facility for automotive research and development. Open jet wind tunnel has become the main form of modern automotive wind tunnel due to its advantages in aerodynamic and aero-acoustic measurement. A well operating wind tunnel must meet the requirement of minimum level for both axial static pressure coefficient and flow pulsation. Axial static pressure coefficient in large value has influence on the measurement accuracy as an additional horizontal force, which is critical for the vehicle aerodynamic force measurement. The high flow field fluctuation not only leads to the instability of the wind speed, but also affects the measurement of the surface pressure and wake flow field. Some researchers have proposed several correction formulas (Mercker and Jochen 1996; Jochen, Oliver and Pang 2004; Mercker, Cooper, Fischer, Wiedemann 2005; Mercker and Cooper 2006) corresponding to the problem of high axial static pressure coefficient for the early wind tunnels.

In order to design a wind tunnel with a low axial variation in static pressure coefficient, researchers have carried out related research from various aspects. Joel *et al.* (Joel, Edward and Bill 2003) carried out experiments to Daimler Chrysler wind tunnel in the conditions of different height, speed as well as the opening and closing of boundary layer control system. He discovered that tangential blowing and distributing suction system only effects the static pressure coefficient 3.5 m to 4.5 m in front of the rotation center, but hardly effects the static pressure coefficient over the rotary balance and behind the body tail. Speed and height have little effect on the static pressure coefficient, which can be ignored. By means of model wind tunnel tests and numerical simulation, Edward *et al.* (Edward and Amir 2010) adopted airfoil collector in the Aerodynamisches Versuchszentrum (AVZ) wind tunnel to improve the boundary-layer control system and eventually obtained a low axial static pressure coefficient. Authors have found that the axial static pressure coefficient can be effectively reduced by increasing the collector angle or increasing the collector throat clearance. By the method of numerical simulation, it is also found that the axial pressure coefficient can be improved by guiding the downstream airflow of test section back to the test section(Li, Zheng, Jia, Yang 2010; Du, Yang, Li 2016).

Low frequency pulsation is a common issue in open jet wind tunnels. It is necessary to control it under a low level. Researchers have developed some effective control measures, which have already been applied in some current wind tunnels (Amandolese and Vartanian 2010; Bergmann, Kaiser, Wagner 2008; Rennie, Kim, Lee, Kee 2004; John 2002; Gerhand, Wilhelm, Steppen 2000; Stephen, Tony, Michael 1999). For example, opening ring in the front of first diffuser and changing the structure of the collector are well-proven means to control the low frequency pulsation. The authors put forward two new control methods: a Helmholtz resonator and addition pipes connected with airline of wind tunnel. They can keep a stable level in entire velocity range and the method of addition airline has been applied to control the low frequency pulsation of the first aerodynamic and aero-acoustic automotive wind tunnel in China (Wang, Yang, Li 2012).

The flow field in the test section is influenced by the auxiliary passage (passive reinjection). Therefore, effects of reinjection in the test section were studied by wind tunnel experiments and numerical simulation. The variations of axial static pressure coefficient, pressure and velocity fluctuations in the test section were assessed for the passive reinjection. For further insight into this issue, active reinjection was introduced through two additional fans. Their influences on the flow field in the test section were also evaluated. The paper is organized as follows: In section 2, the methodology is introduced. In section 3, the results of axial static pressure coefficient, turbulence intensity, velocity and pressure fluctuations are presented.

2. METHODOLOGY

2.1 Wind Tunnel Experiments

A 1:15 scale wind tunnel model was built as the following specification. It is a 3/4 open-jet type, which is usually used in the full scale automotive wind tunnel. The wind tunnel speed is controlled by the fan, and the maximum nozzle speed is 49 m/s. The test section has the dimensions of 1.517 m in length, 1.185 m in width and 0.818 m in height. In order to carry out the research of reinjection, two opening (named as “A” and “E”, respectively) with different sizes are set up from the first diffuser to the corner one and corner two, which is the downstream of the test section. For the purpose of recycling the airflow back to the test section, a loophole is opened above the collector. Therefore, an auxiliary passage can be constructed on the top of wind tunnel to lead the airflow back to the test section from opening “A” and “E”. This kind of reinjection is called passive reinjection because it doesn’t need additional power, as depicted in Fig.1a. Active reinjection introduces external airflow into the wind tunnel by auxiliary fan and exhausts extra air downstream through an opening in the downstream of the test section, is illustrated in Fig.1b. Passive reinjection has the advantage of dispensing with additional power. However, once structure is determined, the flow rate of reinjection is fixed as a constant. On the contrary, active reinjection can adjust the flow rate by changing the fan power, but it needs additional power.

Full scale aerodynamic and aero-acoustic wind tunnel of SAWTC (Shanghai Automotive Wind Tunnel Center) and university of Stuttgart in FKFS are two typical modern advanced automotive wind tunnels. The diffusion angle of them are 3.28° and 1.38°. According to our pervious investigation (Li, Chen, Yang, Xu 2014), when the diffusion angle is below 1.70°, the bigger collector angle becomes, the larger axial static pressure is. On the contrary, when the diffuser angle is above 1.70°, the law is opposite.

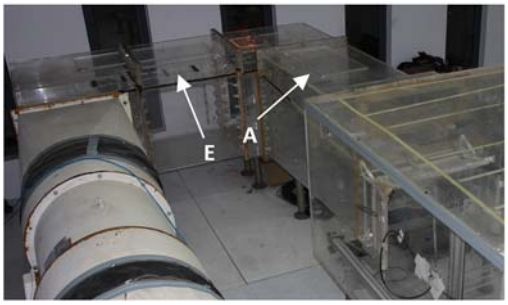

(a) passive reinjection

(b) active reinjection

Fig. 1. Schematic of reinjection structure.

Table 1. Experimental conditions

Diffusion angle	No	Collector angle	0°	15°
3.28°	1	Without reinjection	√	√
	2	Passive reinjection(“A”)	√	√
	3	Passive reinjection(“E”)	√	√
	4	Active reinjection (“2P”)	√	√
	5	Active reinjection (“6P”)	√	√
1.38°	6	Without reinjection	√	√
	7	Active reinjection (“2P”)	√	√
	8	Active reinjection (“6P”)	√	√

In order to further evaluate the influence of diffusion angle to the flow field, a new collector and first diffuser with smaller sectional area were made, and the diffusion angle is 1.38°, as depicted in Fig.1b. Due to the modification of diffusion angle, the structure of auxiliary passage should be modified correspondingly for assembly. On consideration of the limited fund and time, the processing of the auxiliary passage is canceled and the corresponding experiments have not been conducted. Flow characteristics are measured during the experiment for two collector angles and diffusion angles under the conditions of passive reinjection and active reinjection. The experimental conditions are shown in the Tab.1. For the active reinjection, “2P” and “6P” mean the fan power is two blocks and six blocks, respectively. More airflow will be reinjected into the test section when the fan power is “6P”. The nozzle speeds in the experiment are 30 m/s, 35 m/s and 40 m/s.

The averaged static pressure of nineteen measured points is located in the centerline of test section, fifty millimeters above the floor. It starts from the exit of nozzle and ends near the collector and the distance between two points is fifty millimeters. *L* type of Pitot tube is used to measure the average static pressure and the accurate position is controlled by the two-dimensional traversing system. Pressure sensor of SM5852, Silicon Microstructures Inc, converts the pressure signal into electrical signals and is collected by the acquisition system of PMD-1608FS, produced by the Measurement Computing Corporation. Pressure sensor range is ±2000 Pa, and the error is 0.3%FS. Sampling frequency and sampling time are 1024 Hz and 4 s, respectively.

One-dimensional hot wire anemometer is used to measure the mainstream velocity fluctuation at those nineteen measured points after the measurement of averaged static pressure. 55P01 type of hot wire probe, Dantec Dynamics, converts flow velocity signal into electrical signals and is collected by the streamline system, including an automatic calibration system and interface to A/D converter boards. Range of velocity measurement is 0.5~60 m/s and the error is about two percent of measured velocity. Sampling frequency and sampling time are 2000 Hz and 30 s, respectively. When the instantaneous velocity is collected, the root mean square and average of the measured velocity can be calculated, then the turbulence intensity could be obtained for analyzing reinjection.

Pressure fluctuation is measured by two surface microphone sensors of P1 and P2, which are placed on the test section floor at x/L=0 and 1.8, respectively. L is the length of 1:15 scale vehicle and the value is 1/3 meter. 4949 type surface microphone is produced by B&K, and the 95% confidence level is 0.2 dB. An acceleration sensor of P3 is placed on half height of the side wall of the test section to measure the wall vibration. 8776A50M3 type accelerometer has a transverse sensitivity of 0.7%. SQLAB III multi-channel data acquisition system, HEAD acoustics, is used to collect the electrical signal from the surface microphone and accelerometer. The data is analyzed by Artemis 9.0, HEAD acoustics. Sampling frequency and sampling time of surface microphone and accelerometer are 48 kHz and 10 s.

2.2 Numerical Simulation

2.2.1 Flow Simulation Method

The numerical method is used to obtain the flow field detail for the analysis of the aerodynamic mechanism behind the experimental phenomena. Therefore, the numerical simulation is only conducted for several conditions. The wind tunnel model is composed of test section, collector, diffuser, corner, fan motor, honeycomb and contraction section etc, as depicted in Fig. 2a. An auxiliary passage above the pipeline is added when the opening “A” is turned on for passive injection.

The flow field inside the computational domain was discretized by the commercial software of Hypermesh 14.0. All wall surfaces were discretized with triangle mesh elements. The smallest surface element has a size around 2~5 mm, which is located at the surfaces of nozzle, collector and corner vanes. A larger surface element has a size around 10 mm, which is located at the surfaces of test section, diffuser, cross-leg and additional airline. The number of surface mesh is about 3.7 million.

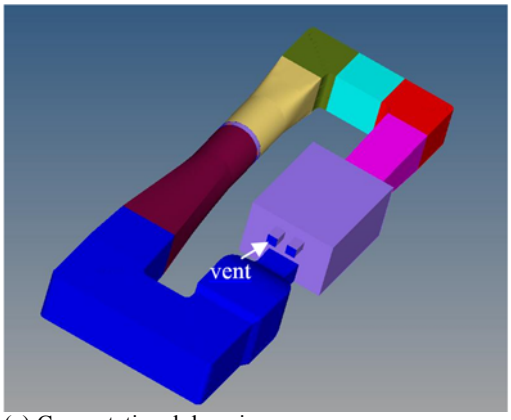

(a) Computational domain

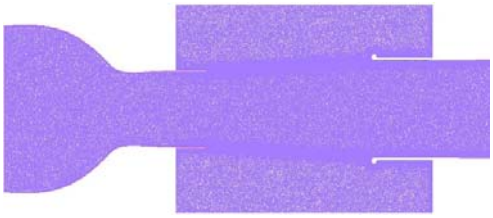

(b) Section grid from the height of test section floor about 50 mm

Fig. 2. Computational model and grid.

Cells of prism layers were created on the wind tunnel component surfaces and the wind tunnel floor to satisfy the required near-wall resolution with y+≈20~200 for better resolving the boundary layer over those surfaces. The remaining volume of the computational domain is filled by tetrahedral cells using commercial software of Fluent 16.1. The number of the cells is strongly dependent on the size of the surface mesh and the size of the computational domain. In the present study, nearly 34 million cells were created in the initial solution. Section grid from the height of test section floor about 50 mm is shown in Fig.2b.

The commercial CFD code Fluent 16.1 was used for the current analysis, and this code is based on finite volume using an unstructured grid. Realizable k-ε model (Shih, Liou, Shabbir, Yang, Zhu 1995) and non-equilibrium wall functions (Launder, Spalding 1974) were used to model the turbulence field. The governing equations are defined as Eq.1~Eq.3

$$\frac{\partial}{\partial t}(\rho k)+\frac{\partial}{\partial x_j}(\rho k u_j)=\frac{\partial}{\partial x_j}[(\mu+\frac{\mu_t}{\sigma_k})\frac{\partial k}{\partial x_j}] + G_k+\mathrm{G_b}-\rho\varepsilon-Y_M+S_k \tag{1}$$

$$\frac{\partial}{\partial t}(\rho\varepsilon)+\frac{\partial}{\partial x_j}(\rho\varepsilon u_j)=\frac{\partial}{\partial x_j}[(\mu+\frac{\mu_t}{\sigma_\varepsilon})\frac{\partial \varepsilon}{\partial x_j}] + \rho C_1 S\varepsilon-\rho C_2\frac{\varepsilon^2}{k+\sqrt{\nu\varepsilon}}+C_{1\varepsilon}\frac{\varepsilon}{k}C_{3\varepsilon}G_b+S_\varepsilon \tag{2}$$

$$C_1=\max[0.43,\frac{\eta}{\eta+5}],\eta = S\frac{k}{\varepsilon},S=\sqrt{2S_{ij}S_{ij}},Sij=\frac{1}{2}(\frac{u_i}{x_j}+\frac{u_j}{x_i}) \tag{3}$$

The fan speed of 1100 rpm can ensure the nozzle speed is 30 m/s and the pressure of vent is set to 0 Pa. Due to the reason of low Mach number of 0.09, an incompressible pressure based solver is used together with an implicit SIMPLE pressure-velocity coupling algorithm. In the computational process, the computation was first carried out with first order scheme for its stability. After two thousand iterations, the computation was switched to the second order scheme to improve numerical accuracy. Grid adaptations were carried out a few times based on the y+ value to guarantee the wall functions are valid. In our cases, the y+ values are mainly in the range of 20~200, which is recommended by Fluent 16.1. The numerical solution is considered as convergence when the residuals for all equations are less than 10^{-5}, as well as the static pressure no longer changes with more iterations.

2.2.2 Modal Calculation

The modal energy of the wind tunnel is overwhelmingly contributed from low frequency. Therefore, only the structural modal frequencies below 100 Hz are concerned in this paper. The wind tunnel surface mesh, which used in the CFD, is directly employed to generate volume mesh for modal calculation. The modal calculation is conducted by finite element software Actran 16.0. Because the computing process of the modal calculation is simple and the result is highly precise, the detail information is not provided in this paper.

3. RESULTS DISCUSSION

3.1 Axial Static Pressure Coefficient

The position of balance center is chosen as the reference point, where x coordinate is equal to zero. We pay close attention to the static pressure coefficient, which is shown as Eq.4.

$$C_{pi}=\frac{p_i-p_{ref}}{p_{0d}} \tag{4}$$

It can be seen from Fig. 3 that the static pressure coefficients of CFD and test have the same trend and close to the value. Both of them show that as x/L becomes larger, the static pressure coefficient decreases slightly and then decreases sharply after x/L = 0.6. When the x/L = 1.95, the static pressure coefficients of the CFD and test are 0.141 and 0.139, respectively. The same trend and small difference indicate that the numerical simulation method is correct.

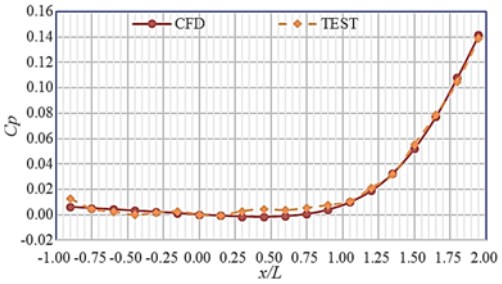

Fig. 3. Comparison of numerical result and test result.

For the conditions of diffusion angle of 3.28° and 1.38° in passive injection, the variation of axial static pressure coefficient alongside the *x*-axis in test section is shown in Fig.4. It should be mentioned that the results presented in follow figures except for Fig.5 are experimental. For the diffusion angle of 3.28°, the axial static pressure coefficient in the back end of test section can be effectively reduced by turning on the opening "A" or "E", whether the collection angle is 0° or 15°. The larger the opening area is, the more air recycle back to the test section, and the greater the static pressure coefficient decreases. For example, when the diffusion angle is 0° and opening "E" is turned on, the static pressure coefficient is only 0.054 at $x/L = 1.95$, while the static pressure coefficient is 0.138 when all the opening is off. When the diffusion angle is 15°, C_{pi} of opening "E" on and all opening off is 0.046 and 0.112, respectively. Moreover, C_{pi} for collector angle of 15° is lower than 0° in the same opening conditions.

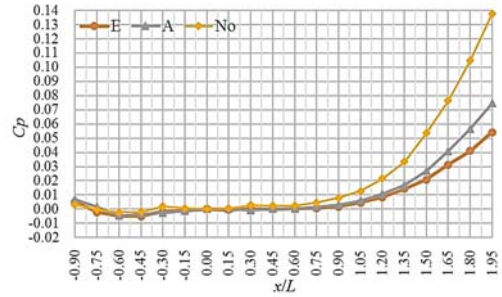

(a) Collector angle is 0° and diffusion angle is 3.28°

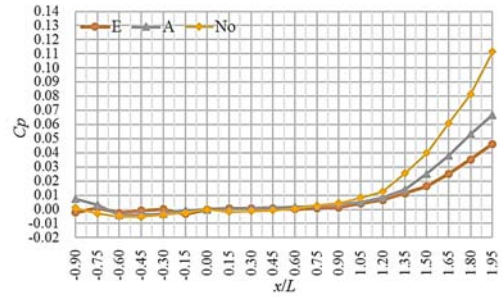

(b) Collector angle is 15° and diffusion angle is 3.28°

Fig. 4. *Cp* curve of passive reinjection.

When the opening "A" is on, part of the diffuser airflow enters the additional passage from opening "A", which is located at the top of diffuser, as depicted in Fig.5. The airflow returns to the test section through the loophole located at the top of collector. Similar processes can be found at other holes. As more airflow returns into the test section through the loophole, the dynamic pressure near collector increases and results in a reduction of static pressure. The reason why opening "E" is better is that the mass flow rate of the loophole is more than that of "A" when the opening is on.

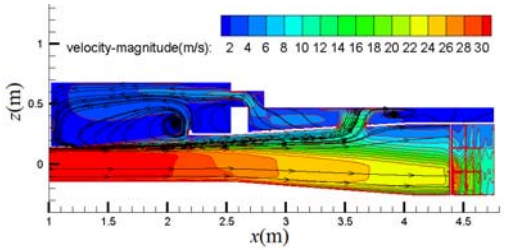

(a) Collector angle is 0°

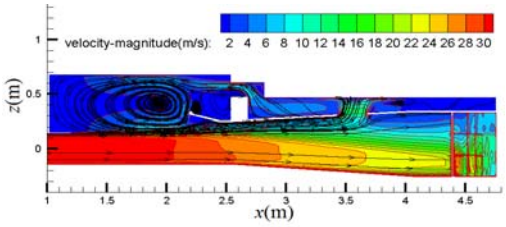

(b) Collector angle is 15°

Fig. 5. Pathlines of test section when the diffusion angle is 3.28°.

In the condition of active reinjection, the axial static pressure coefficient in the test section for the cases of 3.28° and 1.38° is shown in Fig.6. For the diffusion angle of 3.28°, the axial static pressure coefficient in the back end of the test section can be effectively reduced in the condition of active reinjection, where the external airflow is injected into the test section through an additional fan and extra air inside the wind tunnel flows out through opening "E", whether the collector angle is 0° or 15°. When the collector angle is 0°, the static pressure coefficient near the collector outlet can be further reduced by increasing the fan speed i.e. the flow rate of injected airflow. When the diffusion angle is 3.28°, because the static pressure coefficient near the collector is much larger than that near the nozzle, it is advantageous to reduce the static pressure coefficient near the collector for aerodynamic force measurement. However, in the condition of diffusion angle of 1.38°, the variation of static pressure coefficient alongside the *x* axis in test section is small. In this circumstance, the reduction of C_{pi}, which happens in the condition of active reinjection, is unfavorable for aerodynamic force measurement. When the collector angle is 15°, the increasing the fan speed has no major impact on C_{pi}. Because C_{pi} near the collector is positive in the conditions of 15° collector angle for both diffuser angles, active reinjection is beneficial to the aerodynamic measurement. It is worth noting that when diffusion angle is 1.38°, C_{pi} at $x/l = 1.95$ corresponding to the collector angle of 15° is higher than that of 0°, which

is contrary to the tendency of the diffusion angle of 3.28°. In both diffusion angles, when the collector angle is 0° and active reinjection is on, C_{pi} in the back end of the test section decreased more than the one corresponding to the collector angle of 15°.

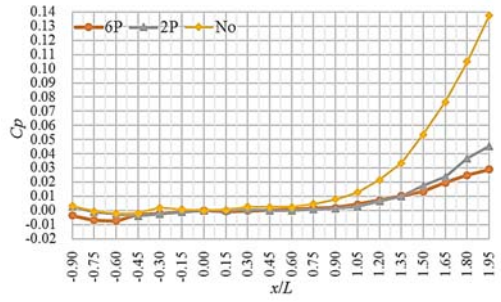

(a) Collector angle is 0° and diffusion angle is 3.28°

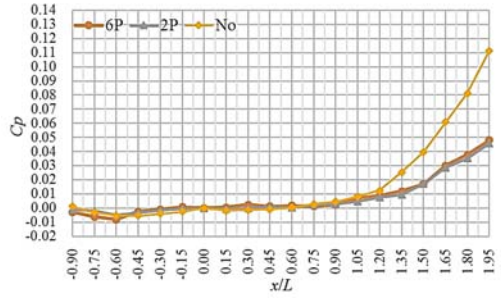

(b) Collector angle is 15° and diffusion angle is 3.28°

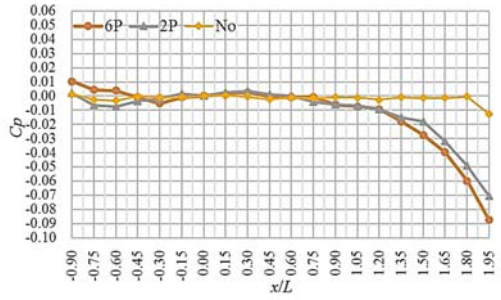

(c) Collector angle is 0° and diffusion angle is 1.38°

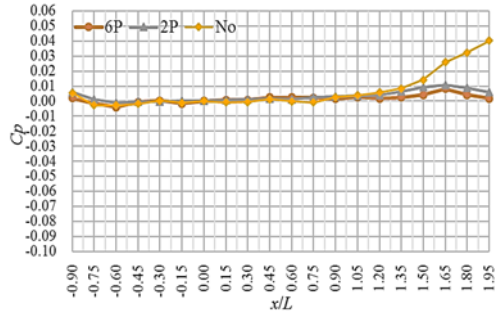

(d) Collector angle is 15° and diffusion angle is 1.38°

Fig. 6. *Cp* curve of active reinjection.

3.2 Velocity Fluctuation

3.2.1 Turbulence Intensity

All of the pervious discussions are focused on the axial static pressure coefficient, which is a time averaged flow field characteristic. As a matter of fact, we should concern the fluctuation flow field because high turbulence intensity leads to the vibration of equipment and reduces the accuracy of test.

For the diffusion angle of 3.28°, both passive reinjection and active reinjection will increase the turbulence intensity near the collector, as depicted in Fig.7. It can be found that when the collector angle is 0°, the turbulence intensity is larger than that of the collector angle of 15°, and the influence of passive reinjection on the collector angle of 0° is greater than that on the collector angle of 15°. For example, for the collector angle of 0°, the turbulence intensity at $x/l = 1.8$ increases 0.38 for passive reinjection, while the one of the collector angle of 15° only increases 0.08. The tendency of active reinjection is the same as the passive one. When the diffusion angle is 1.38°, it is also found that active reinjection increases the turbulence intensity while the increment of 15° collector angle is larger.

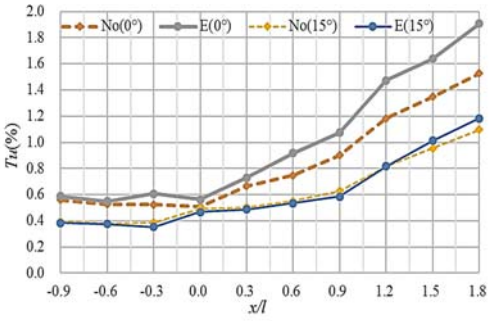

(a) Passive reinjection at the diffusion angle of 3.28°

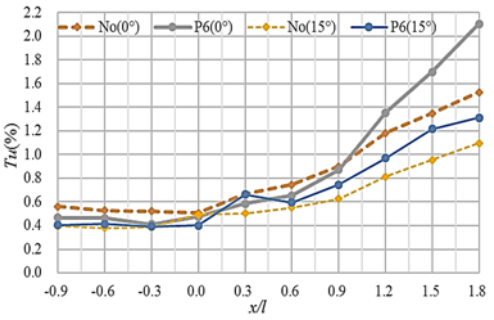

(b) Active reinjection at the diffusion angle of 3.28°

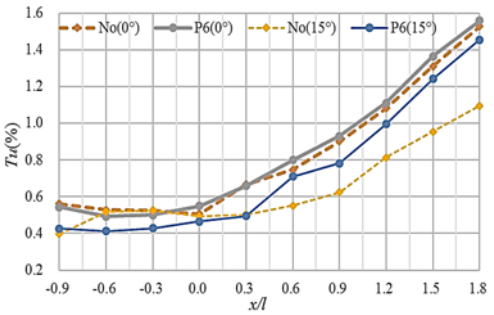

(c) Active reinjection at the diffusion angle of 1.38°

Fig. 7. Turbulence intensity.

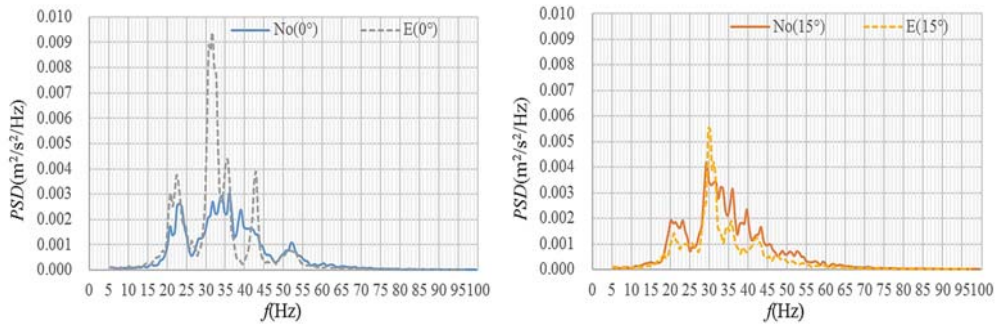

(a) Passive reinjection at the diffusion angle of 3.28°

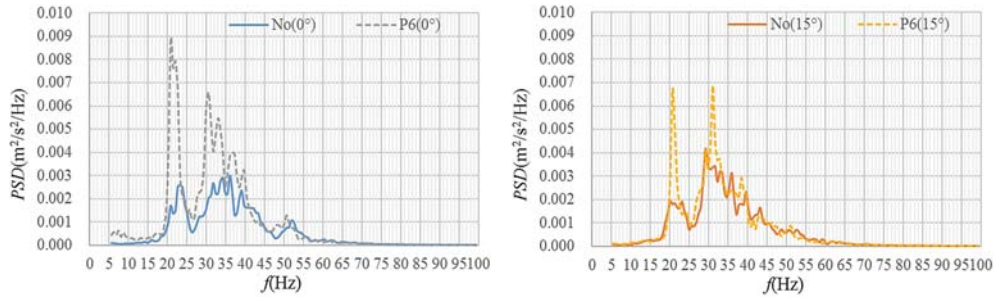

(b) Active reinjection at the diffusion angle of 3.28°

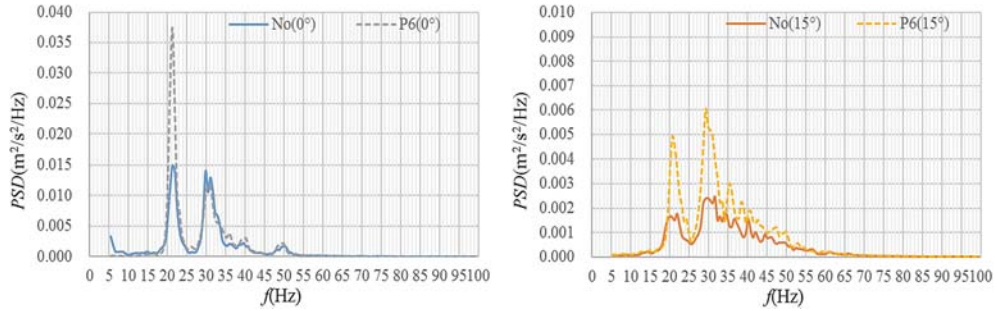

(c) Active reinjection at the diffusion angle of 1.38°

Fig. 8. PSD of velocity fluctuation.

3.2.2 Power Spectral Density

The velocity of measured point at x/l = 1.2 is selected for power spectral density (PSD) analysis, as depicted in Fig.8. In the condition of passive reinjection, it is found that the energy of several frequencies increase for the collector angle of 0°. The largest increment is 0.006 that occurs at the frequency of 31 Hz. However, the energy of another case, which has the collector angle of 15°, increased slightly at this frequency by only 0.001. In the condition of active reinjection, whether the diffusion angle is large or small, reinjection would be the main cause of the growth of velocity fluctuation, especially for some typical frequencies such as 21 Hz and 31 Hz. It can still be found that the influence of reinjection for the case of 0° collector angle is greater than that of 15°.

3.3 Pressure Fluctuation

Because the pressure fluctuation and vibration energy of these measured points are small at middle and high frequencies, the PSD is shown only below 100 Hz in Fig.9. Since only the energy below 100 Hz is concerned, it can be considered that the main contribution is turbulence fluctuation, which is called as hydrodynamic pressure fluctuation. In Fig. 8a, the vertical axis of P2 is the primary axis, while the vertical axis of P1 is the secondary axis. In Fig. 8b, the vertical axis of P3 is the primary axis, while the one of P2 is the secondary axis. It can be seen from Fig. 8a that the peak frequencies of two curves are basically the same, which are 7 Hz, 17 Hz, 31 Hz, 40 Hz and 50 Hz. However, the quantities of among these peaks between the two curves have large differences. The value of the P2 near the collector is much larger than the one of the point P1. For instance, the value of the P2 at the frequency of 17 Hz is 1.24, while the one of the P1 is only 0.023. Because the reinjection has the greatest impact on the collector when it locates the top of the collector, the following analysis is major

concerned about P2, which locates near the collector. It can be seen from Fig.8b that, peaks appear at the frequency of 31 Hz, 40 Hz, 50 Hz both for the pressure fluctuation of P2 and the acceleration of P3. Since P2 is located in the test section and P3 is located on the wall of wind tunnel, it may indicate that the flow field fluctuations are the factors that lead to structural resonance. For the purpose of further insight into this phenomenon, modal calculation of the wind tunnel structure is conducted. The modal frequencies are shown in Table 2. It can be seen from the table that the 3rd and the 4th ordered modes of the wind tunnel structure are correlate with jet shear layer. The cause why peak appears at the frequency of 31 Hz is still unclear yet. As for the frequencies of 7 Hz and 17 Hz, where appears the peaks for pressure fluctuation, they might be the frequencies corresponding to the big vortex structure produced by the interaction between the jet shear layer and the collector.

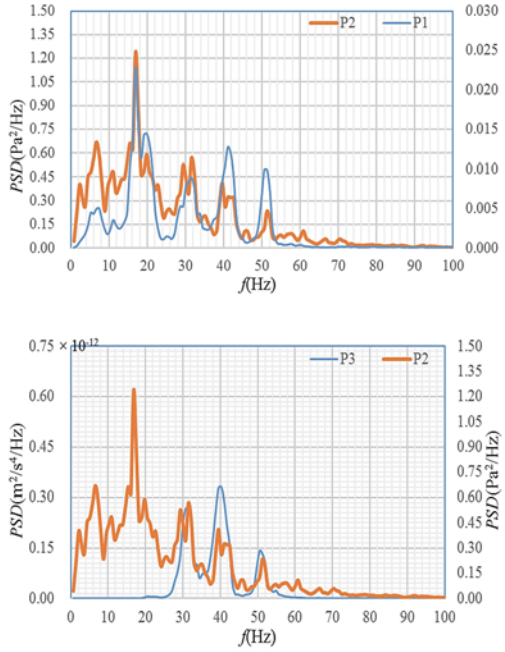

Fig. 9. *PSD* of measured points at the collector angle of 0° and diffusion angle of 3.28°.

Table 2 Modal frequency

Order	1	2	3	4	5	6	7	8
f (Hz)	19	23	39	49	63	77	90	96

Figure10a and Fig.10b show the PSD of the wall acceleration and pressure fluctuation measured at different wind speeds for P3 and P2, respectively. It can be seen from Fig.10a that when wind speed increases from 30 m/s to 35 m/s, energy at 40 Hz increases sharply and becomes the major contribution. When the speed increases to 40m/s, the energy decreases a lot at 40 Hz, which reduces from 2.34x 10^{-12} to 0.93x 10^{-12}. It is less than the energy at 50 Hz. At the speed of 40 m/s, in addition to the three frequencies mentioned above, there are several other peaks emerged with close value, which indicates that the energy distribution is more diverse. But the maximum energy still locates near 50 Hz with the value of 2.66. However, at the wind speed of 35 m/s, the energy at 40Hz is much larger than the one at 17 Hz with the difference of 1.32. The wind speed of 30m/s is most typical for wind tunnel design and test, and most of the frequency characteristics in this speed. Therefore, 30 m/s is selected for the following analysis of the reinjection effects.

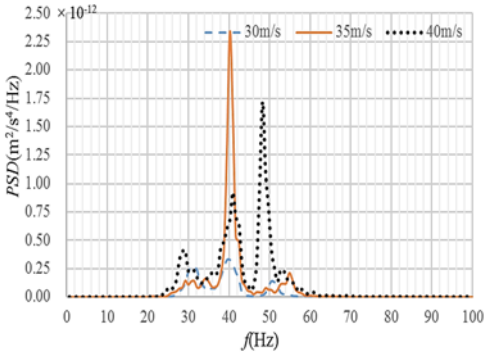

(a) P3

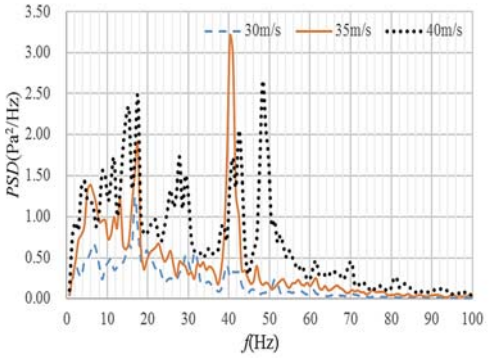

(b) P2

Fig. 10. *PSD* of measured points at the collector angle of 0° and diffusion angle of 3.28°.

When the diffusion angle is 3.28°, effects of passive reinjection on the pressure fluctuation in test section are shown in Fig.11. It is found that reinjection has caused changes to the flow field in test section. Energy of several peak frequencies is reduced by reinjection, while the values for most other frequencies increase. The higher the flow rate of reinjection is, the larger the value will be. For example, when the collector angle is 0° and hole "E" is opened, energy at the frequencies of 31 Hz and 40 Hz increases by 0.28 and 0.68 comparing with no reinjection. Similar tendency also occurs when the collector angle is 15°. It is should be noticed that, in the conditions without reinjection, energy at 17 Hz on the collector angle of 15° is much lower than that on the collector angle of 0°, so the pressure fluctuation at a lower level occurs. However, when reinjection is conducted, energy at several frequencies on the collector of 15° is higher than that of 0°, which

indicates a much higher level of pressure fluctuation. The high level of pressure fluctuation has negative impacts on flow field measurement. For instance, energy at 31 Hz on the collector angle of 15° increases by 0.6 comparing with the one when the collector angle is 0°.

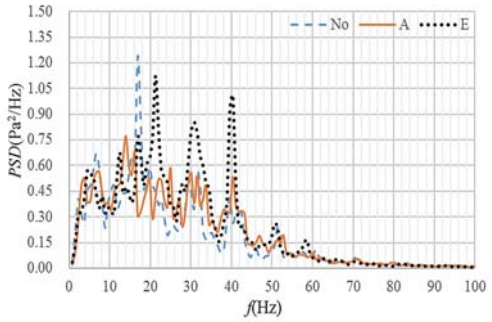

(a) Collector angle is 0° and diffusion angle is 3.28°

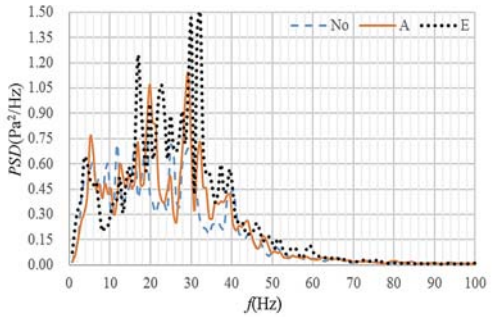

(b) Collector angle is 15° and diffusion angle is 3.28°

Fig. 11. *PSD* of passive reinjection.

As for the diffusion angle of 3.28° and 1.38°, effect of active reinjection on the pressure fluctuation in test section is shown in Fig.12. Active reinjection intensifies the pressure fluctuation in the test section for both diffusion angles. The increase of reinjection flow rate will coherently increase the energy of pressure fluctuation. When the diffusion angle is 3.28° and the collector angle is 0°, effects of active reinjection are more obvious and the peak energy is more prominent. For example, in the conditions of P2 and P6, the peak values at 30 Hz increase by 0.4 and 1.2, respectively. When the collector angle is 15°, effects of active injection are not obvious, where energy at most frequencies increases slightly. The peak energy is slightly reduced with the increase of reinjection flow rate at several frequencies. Thus, active reinjection on the collector angle of 15° has less negative impact. When the diffusion angle is 1.38° and the collector angle is 0°, effects of active reinjection are more obvious. Energy increased much more than the diffusion angle of 3.28°. It not only largely increased at the maximum peak frequency, but also increased at the second peak frequency of 40 Hz. When the collector angle is 15°, energy near 40 Hz is not obvious and the increase of energy at 31 Hz is not large.

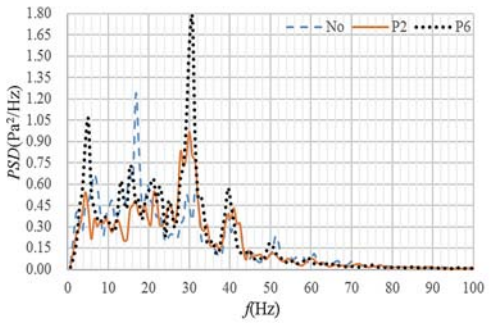

(a)Collector angle is 0° and diffusion angle is 3.28°

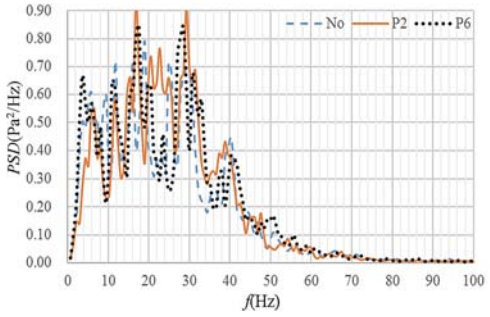

(b) Collector angle is 15° and diffusion angle is 3.28°

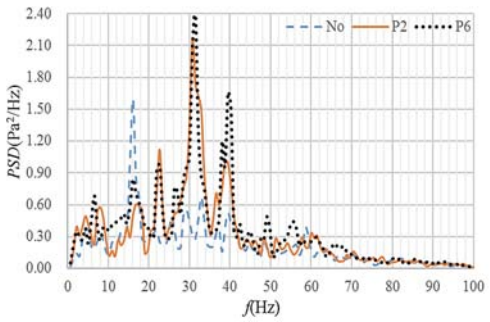

(c) Collector angle is 0° and diffusion angle is 1.38°

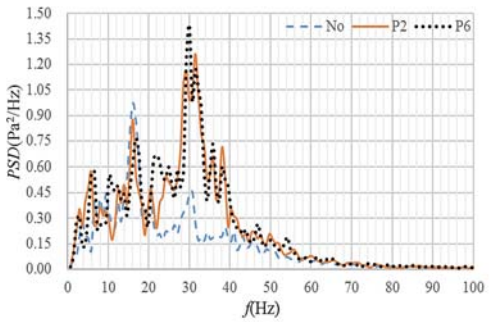

(d) Collector angle is 15° and diffusion angle is 1.38°

Fig. 12. *PSD* of active reinjection.

4. CONCLUSION

The effects of reinjection on flow field of open jet automotive wind tunnel test section were investigated by wind tunnel test together with numerical simulation. Axial static pressure coefficient, turbulence intensity, velocity and pressure fluctuations were measured by Pitot tube,

hot wire anemometer and surface microphone under different diffusion angles and collector angles. The research shows that:

(1) The axial static pressure coefficient in the rear end of test section can be reduced by passive or active reinjection. The airflow returned to the test section through loophole and the mass flow rate of loophole are the main factors to decide the improvement effect of the axial static pressure coefficient.

(2) For large diffusion angle such as 3.28°, the maximum static pressure coefficient near the collector angle of 0° is higher than that of the angle of 15°. For small diffusion angle such as 1.38°, the tendency is the contrary. However, it is found in the experiment that the improvement of the axial static pressure coefficient by reinjection is always better in the condition of 0° collector angle.

(3) The turbulence intensity at measured point in the case of the collector angle of 15° is lower than that of 0°. The reinjection increases the turbulence intensity near the collector. For the larger diffusion angle, the increase of the turbulence intensity by active reinjection in the collector angle of 0° is greater than that of 15°, which is contrary to the tendency of the smaller diffusion angle.

(4) For the quantity of pressure fluctuation, velocity fluctuation and wall acceleration, it is discovered from the spectral analysis that peaks emerge at same the frequencies of 40 Hz and 50 Hz, which indicates that the flow field fluctuations may have induced structural vibration. Through modal calculation, it is suggested that the wind tunnel structure may be in resonance with the flow field fluctuations, which is the result of interaction between shear layer vortex shedding and collector.

(5) For both passive and active reinjections, the peaks at several frequencies increase. The increase of peak is correlate with the increase of the reinjection flow rate. The reinjection is beneficial for the reduction of average static pressure coefficient in the rear end of test section, but it leads to the increase of velocity and pressure fluctuations, which deteriorates the unsteady flow field. Therefore, for the future of wind tunnel design and vehicle test, the most suitable control method is determined by the measurement demand. The study of its effect on acoustic field in the test section is complex but worthy to investigate.

ACKNOWLEDGEMENTS

The authors gratefully acknowledge the National Natural Science Foundation of China under the Grants No 11502171 and the Project of professional and technical services platform under the Grants No 16DZ2290400.

REFRENCES

Amandolese, X. and C. Vartanian (2010). Reduction of 3/4 open jet low-frequency fluctuations in the S2A wind tunnel. *Journal of Wind Engineering and Industrial Aerodynamics* 98(10-11), 568-574.

Bergmann, D., U. Kaiser and S. Wagner (2008). Reduction of low-frequency pressure fluctuations in wind tunnels. *Journal of Wind Engineering and Industrial Aerodynamics* 91(4), 543-550.

Du, K. Y., Z. G. Yang and Q. L. Li (2016).The effects of re-injecting from the airline on the axial static pressure coefficient Computer Aided Engineering. 25(3), 40-46

Edward, D. and K. Amir (2010). The BMW AVZ wind tunnel center. *SAE Technical* 01-0118.

Gerhand, W., V. H. Wilhelm and W. Steppen (2000). Wind tunnel pulsation and their active suppression.*SAE* 2000-01-0869.

Jochen, W., F. Oliver and J. B. Pang (2004). Further investigations on gradient effects. *SAE* 2004-01-0670.

Joel, W., D. Edward and M. Bill (2003). The Daimler Chrysler full scale aero acoustic wind tunnel. *SAE Technical* 2003-01-0426.

John, L. (2002). A study of the pulsations in a 3/4 open jet wind tunnel. *SAE* 2002-01-0251.

Launder, B. E., D. B. Spalding (1974). The numerical computation of turbulent flows. *Computer Methods in Applied Mechanics Engineering* 3(2), 269-289.

Li, Q. L., L. Chen, Z. G. Yang and Y. D. Xu (2014). Study on the axial static pressure coefficient of automotive wind tunnel test section at different diffuser angles. *Journal of Tongji university (natural science)* 42(8), 1227-1230.

Li, Q. L., Z. Q. Zheng, Q. Jia and Z. G. Yang (2010) .Study on two methods to improve the axial static pressure coefficient of automotive wind tunnel.*Journal of Tongji university (natural science)* 38(3), 422-426.

Mercker, E., K. Cooper, O. Fischer and J. Wiedemann (2005). The influence of a horizontal pressure distribution on aerodynamic drag in open and closed wind tunnels. *SAE* 2005-01-0867.

Mercker, E. and K. R. Cooper (2006). A two-measurement correction for the effects of a pressure gradient on automotive open-Jet wind tunnel measurements. *SAE* 2006-01-0568.

Mercker, E. and W. Jochen (1996). On the correction of interference effects in open jet wind tunnels. *SAE 960671*.

Rennie, M., M. Kim, J. Lee and J. Kee (2004). Suppression of open-jet pressure fluctuations in the Hyundai aero-acoustic wind tunnel. *SAE*

2004-01-0803.

Shih, T. H., W. W. Liou, A. Shabbir, Z. Yang and J. Zhu (1995). A new *k-ε* eddy viscosity model for high Reynolds number turbulent flows: model development and validation. *Computers and Fluids* 24(3), 227-238.

Stephen, A. A., D. B. Tony and Z. Michael (1999). On low frequency pressure pulsations and static pressure distribution in open jet automotive wind tunnels. *SAE paper* 1999-01-0813.

Wang, Y. G., Z. G. Yang and Q. L. Li (2012). Methods to control low frequency pulsation in open jet wind tunnel. *Applied Acoustics* 73(6-7), 666-672.